

**Programmable two-photon quantum interference in  $10^3$  channels in opaque scattering media**Tom A. W. Wolterink,<sup>1,2,\*</sup> Ravitej Uppu,<sup>1</sup> Georgios Cstis,<sup>1,3</sup> Willem L. Vos,<sup>1</sup> Klaus-J. Boller,<sup>2</sup> and Pepijn W. H. Pinkse<sup>1,†</sup><sup>1</sup>*Complex Photonic Systems (COPS), MESA+ Institute for Nanotechnology, University of Twente, P.O. Box 217, 7500 AE Enschede, The Netherlands*<sup>2</sup>*Laser Physics and Nonlinear Optics (LPNO), MESA+ Institute for Nanotechnology, University of Twente, P.O. Box 217, 7500 AE Enschede, The Netherlands*<sup>3</sup>*NanoBioInterface, Saxion University of Applied Sciences, P.O. Box 70000, 7500 KB Enschede, The Netherlands*

(Received 30 October 2015; published 11 May 2016)

We investigate two-photon quantum interference in an opaque scattering medium that intrinsically supports a large number of transmission channels. By adaptive spatial phase modulation of the incident wave fronts, the photons are directed at targeted speckle spots or output channels. From  $10^3$  experimentally available coupled channels, we select two channels and enhance their transmission to realize the equivalent of a fully programmable  $2 \times 2$  beam splitter. By sending pairs of single photons from a parametric down-conversion source through the opaque scattering medium, we observe two-photon quantum interference. The programmed beam splitter need not fulfill energy conservation over the two selected output channels and hence could be nonunitary. Consequently, we have the freedom to tune the quantum interference from bunching (Hong-Ou-Mandel-like) to antibunching. Our results establish opaque scattering media as a platform for high-dimensional quantum interference that is notably relevant for boson sampling and physical-key-based authentication.

DOI: [10.1103/PhysRevA.93.053817](https://doi.org/10.1103/PhysRevA.93.053817)**I. INTRODUCTION**

Light waves propagating through an opaque scattering medium exhibit a random walk inside the medium, which is caused by multiple scattering from spatial inhomogeneities [1]. An alternative description describes this by a transmission matrix [2,3]. The transmission matrix describes how a large amount of input channels is coupled to a similarly large amount of output channels, see Fig. 1. The number of these channels can be controlled, and easily made to exceed millions, by increasing the illuminated area on the medium. Recent advances in the control of light propagation through wavefront shaping allow for complete control over these channels in multiple-scattering media [3–5]. Because of their large number of controllable channels, we explore the use of multiple-scattering media to study quantum interference between multiple photons. Employed as a platform for high-dimensional quantum interference, over a large number of channels, multiple-scattering media are of relevance to boson sampling [6–14], quantum information processing [15–18], and physical-key-based authentication [19].

It has previously been observed that quantum states are robust against multiple scattering. Correlations in two-photon speckle patterns in single-scattering media have been studied [20,21]. Further, propagation of quantum noise [22–24] and propagation of single-photon Fock states through multiple-scattering media [25,26] have also been explored. So far it has remained an open question if quantum interference of multiple photons could be demonstrated inside a multiple-scattering medium. A hurdle one might expect in an experimental implementation is the low transmission of almost all channels in the multiple-scattering medium. Remarkably, the transmission per

channel is not necessarily low since wavefront shaping allows funneling of light into selected output modes [3,5].

Here we report on an experiment in which we study quantum interference in a multiple-scattering medium. We observe quantum interference of pairs of single photons in a programmable  $2 \times 2$  beam splitter [27,28], made of a multiple-scattering medium and a spatial light modulator (SLM). The SLM controls  $10^3$  optical channels that are coupled in a reproducible yet unpredictable way in the multiple-scattering medium. The wavefront-shaping technique using the SLM allows us to select two output channels out of  $N$  by enhancing the amplitude of light transmitted in these channels. Programmability in this beam splitter is achieved by controlling the relative phase between the input and output arms, unlike a conventional beam splitter. We exploit this property to demonstrate not only the well-known Hong-Ou-Mandel-like bunching [29], but also the antibunching of the outgoing photon pairs, as well as any intermediate situation. Our result establishes opaque scattering media as a platform for high-dimensional quantum interference experiments as needed in, e.g., boson sampling. At present we control about  $10^3$  channels, but this can readily be scaled up to a number comparable to the number of pixels in modern SLMs of order  $10^6$ .

**II. EXPERIMENTAL SETUP**

Pairs of single photons in our experiment are generated using collinear Type-II spontaneous parametric down-conversion (SPDC) with a mode-locked pump at wavelength centered at 395 nm [25,30,31] as shown in Fig. 2(a) (see Supplemental Material in Ref. [32]). The two orthogonally polarized single photons ( $\lambda_c = 790$  nm) are separated using a polarizing beam splitter (PBS) and coupled into single-mode fibers (SMFs). The temporal delay between the two photons can be controlled with a linear delay stage in one of the single-photon channels. To measure the degree of indistinguishability of the two photons, we observe Hong-Ou-Mandel (HOM) interference

\*t.a.w.wolterink@utwente.nl

†p.w.h.pinkse@utwente.nl

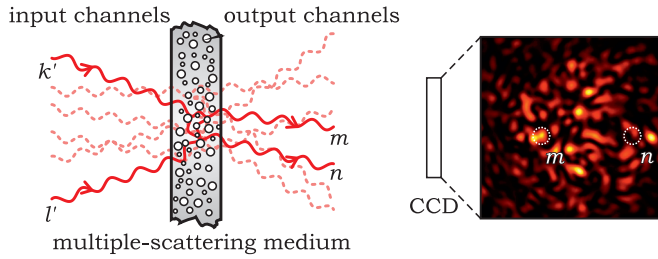


FIG. 1. A multiple-scattering medium couples millions of input and output channels. Light incident in the input channels results through multiple scattering in a complex interference pattern (speckle: see right panel) at the output, which can be imaged by a CCD camera. Each speckle spot in the image corresponds to an independent output channel. In this work we have programmed their interaction to create a network with two inputs ( $k'$ ,  $l'$ ) and two outputs ( $m$ ,  $n$ ).

at a conventional 50:50 beam splitter as shown in Fig. 2(b). At a pump power of 10 mW, a HOM dip with a visibility of 64% is observed (cyan squares), with the usual definition of the visibility of  $V \equiv (R_{\text{indist}} - R_{\text{dist}})/R_{\text{dist}}$ , where  $R_{\text{dist}}$  and  $R_{\text{indist}}$  are the coincidence rates of distinguishable and indistinguishable photons, respectively. The visibility is less than unity due to a residual spectral distinguishability of the two photons allowed by the SPDC process. To improve the spectral indistinguishability, a bandpass filter with a bandwidth of 1.5 nm was used that resulted in a HOM dip with an

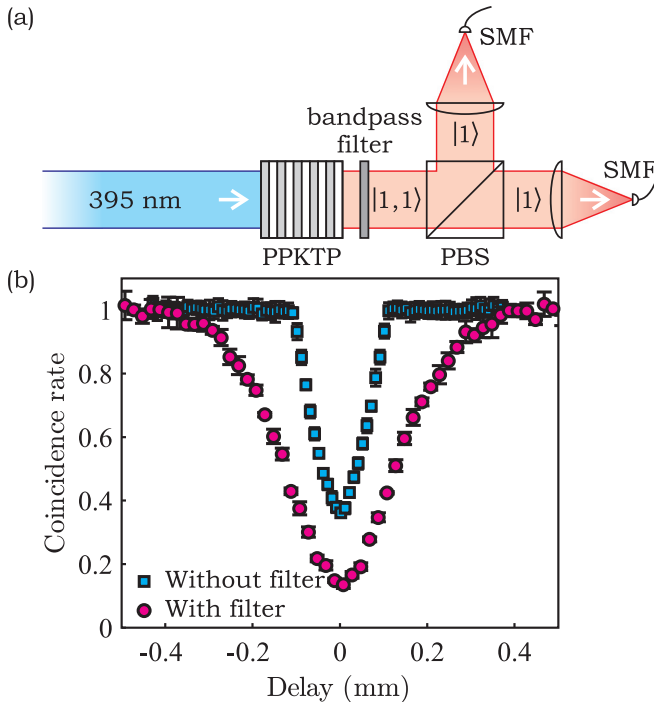


FIG. 2. Our quantum-light source. (a) Photon pairs generated in a periodically poled potassium titanyl phosphate crystal (PPKTP) are separated by a PBS and coupled into SMFs. The photons can be frequency filtered by inserting a bandpass filter. (b) Measured HOM interference without a bandpass filter (cyan squares) and with a bandpass filter (magenta circles). Error bars indicate the standard deviation in the measurements.

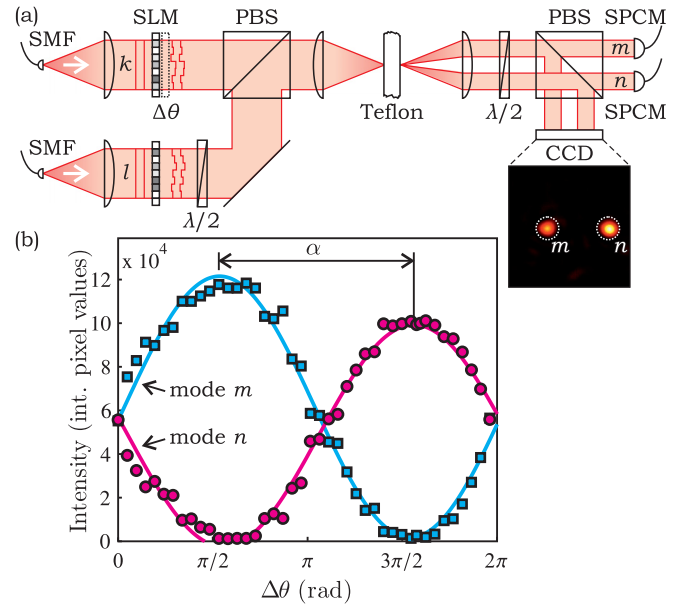


FIG. 3. Wavefront-shaping setup for programming quantum interference. (a) Two input modes ( $k$ ,  $l$ ) are modulated with a SLM, spatially overlapped with orthogonal polarizations, and focused on a layer of Teflon. The transmitted light is either projected onto a CCD, or onto two fibers connected to SPCMs which are selectively observing two output modes ( $m$ ,  $n$ ). (b) Interference between the input modes onto the output modes  $m$  (cyan) and  $n$  (magenta). The solid curves indicate sine fits to the data, resulting in  $\alpha = 1.02\pi$ .

increased visibility of 86% (magenta circles). The decrease in the spectral width also increases the width of the HOM dip as is evident in the figure.

To demonstrate programmable quantum interference in a multiple-scattering medium, we direct the light from the quantum-light source to a wavefront-shaping setup with two SMFs as shown in Fig. 3(a). The two fiber outputs have identical polarization and beam waist and form the input modes  $k$  and  $l$  for the quantum interference experiment. Both modes are phase modulated with a liquid-crystal SLM, and afterwards spatially overlapped using a half-wave plate and a PBS, resulting in a collinear propagation of the two modes with orthogonal polarizations. The orthogonal input polarizations ease the process of creating multiport circuits using wavefront shaping [28]. The multiple three-dimensional scattering within the medium results in an unpolarized speckle pattern, on average. However the degree of polarization is preserved within each speckle [33,34]. Using wavefront shaping the transmitted light can be projected into any chosen polarization [35]. An objective (NA = 0.95, where NA stands for numerical aperture) is used to focus the light onto the scattering medium which is comprised of a 500- $\mu\text{m}$ -thick layer of polytetrafluoroethylene (PTFE, Teflon), with a scattering mean free path of  $150 \pm 10 \mu\text{m}$  (coherent backscattering measurement). The experimental setup, including the multiple-scattering medium, is interferometrically stable for a duration longer than a month. The transmitted light is collected by an objective (NA = 0.6) and after transmission through a PBS it is coupled into two multimode fibers (output modes  $m$  and  $n$ ) connected to single-photon counting modules (SPCMs). This PBS ensures that the

output modes have the same, well-defined linear polarization. The fibers have a core diameter of  $200\ \mu\text{m}$ , which is smaller than the size of a single speckle in the transmitted light. This ensures light collection from only a single mode. The total number of contributing modes (speckles)  $N$  is approximately  $10^4$ . By rotating a half-wave plate this light can also be reflected off the PBS and projected onto a CCD camera for wavefront shaping.

Realization of a programmable  $2 \times 2$  beam splitter inside a scattering medium follows a wavefront-shaping process. To ease this process, we couple classical laser light ( $\lambda_c = 790\ \text{nm}$ ) into the SMFs and monitor the light in the output modes using amplified photodiodes. In short, the process starts with a single input mode  $k$  incident on the scattering medium. We optimize the output mode  $m$  by fitting the optimal phase for each SLM segment that results in maximum constructive interference in the fiber [4]. Each input mode is controlled by approximately 960 segments on the SLM. The average intensity of each output mode before optimizing is  $1/N$ , i.e., all output modes are nearly equiprobable for single photons. For our experimental setup with  $N \approx 10^4$ , we estimate the coincidence detection rate in a photon correlation measurement between two modes at only  $0.02^2(1/N)^2 10^6\ \text{s}^{-1} = 4 \times 10^{-6}\ \text{s}^{-1} \approx 1/(3\ \text{days})$ , considering a photon-pair generation rate of  $10^6\ \text{s}^{-1}$  and an effective detection probability of 2% (all optical losses in the setup and detector efficiencies) (see Supplemental Material in Ref. [32]). After optimizing, the intensity of the enhanced output mode coupled to the fiber is about 200 times higher, i.e., the sampling probability of this mode is  $200/N$ . In photon correlation measurements, this enhancement would result in an increase of  $10^4$  in coincidence detection rates, now giving coincidence detection rates of  $0.04\ \text{s}^{-1} \approx 100\ \text{h}^{-1}$ . We optimize the second output mode  $n$  in the same way. A camera image of two optimized output modes is shown in Fig. 3(a). This optimization procedure is repeated for the input mode  $l$ , resulting in four phase patterns. By combining these four interference patterns we can program any  $2 \times 2$  circuit [28].

### III. MODEL

The transmission through the circuit in this experiment is described by the following equation that relates the electric field of the two output modes,  $E_m$  and  $E_n$ , to that of the two input modes,  $E_k$  and  $E_l$ , through the transmission matrix  $\mathbf{T}$ :

$$\begin{bmatrix} E_m \\ E_n \end{bmatrix} = \mathbf{T} \begin{bmatrix} E_k \\ E_l \end{bmatrix} = t \begin{bmatrix} 1 & 1 \\ 1 & \exp(i\alpha) \end{bmatrix} \begin{bmatrix} E_k \\ E_l \end{bmatrix}, \quad (1)$$

where the parameter  $\alpha$  is set in the algorithm when combining the interference patterns. The amplitude transmission coefficient  $t$  has  $|t| < 1/\sqrt{2}$ , emphasizing that the circuit is inherently lossy for the selected output modes. Since the two selected modes stem from a manifold of  $N$  modes, the programmed  $2 \times 2$  circuit need not fulfill energy conservation and could thus be nonunitary. Only for  $\alpha = \pi$  and  $|t| = 1/\sqrt{2}$  do we have a unitary matrix with  $\mathbf{T}^\dagger \mathbf{T} = 1$ , and this transmission matrix represents an ideal 50:50 beam splitter. To confirm the functionality of each circuit, classical light is injected into both input modes  $k$  and  $l$  and the intensities of the output modes  $m$  and  $n$  are monitored while applying a phase difference  $\Delta\theta$  between the input modes. An example of such an interference

measurement is shown in Fig. 3(b) for  $\alpha = \pi$ . A similar measurement at  $\alpha = 0$  shows two overlapping  $(1 + \sin \Delta\theta)$ -shaped curves, indicating the inherent nonunitary behavior of this  $2 \times 2$  circuit. After programming the functionality, we switch back from classical light to single photons.

Quantum mechanically, the circuit of Eq. (1) can be described using ladder operators  $\hat{a}$  as follows:

$$\begin{bmatrix} \hat{a}_m \\ \hat{a}_n \end{bmatrix} = \mathbf{T} \begin{bmatrix} \hat{a}_k \\ \hat{a}_l \end{bmatrix} + \begin{bmatrix} \hat{F}_m \\ \hat{F}_n \end{bmatrix}, \quad (2)$$

where  $\hat{F}_m$  and  $\hat{F}_n$  are the Langevin noise operators that model the losses in the selected output modes [36,37]. These losses also include the residual intensity in unmonitored modes. Writing the input of the circuit described by Eq. (2) as  $\Psi_{\text{in}} = |1\rangle_k |1\rangle_l$ , one can find the probabilities for all possible outputs in a straightforward manner [36] for indistinguishable photons:

$$\begin{aligned} P(2_m, 0_n) &= P(0_m, 2_n) = 2|t|^4, \\ P(1_m, 1_n) &= 2|t|^4(1 + \cos \alpha), \\ P(1_m, 0_n) &= P(0_m, 1_n) = 2|t|^2 - 2|t|^4(3 + \cos \alpha), \\ P(0_m, 0_n) &= 1 - 4|t|^2 + 2|t|^4(3 + \cos \alpha). \end{aligned} \quad (3)$$

Of interest are the probabilities  $P(2_m, 0_n)$ ,  $P(0_m, 2_n)$ , and  $P(1_m, 1_n)$ , for which both photons arrive in output modes  $m$  and  $n$ . As evident from  $P(1_m, 1_n)$ , we have the freedom to program the quantum interference from bunching (Hong-Ou-Mandel-like) to antibunching by tuning  $\alpha$ . The contribution of the unmonitored modes shows up as the nonzero probabilities  $P(1_m, 0_n)$ ,  $P(0_m, 1_n)$ , and  $P(0_m, 0_n)$ , which account for losses of photons in the output modes  $m$  and  $n$ .

### IV. RESULTS

Using the circuit of Fig. 3(b) programed with  $\alpha = \pi$ , representing a 50:50 beam splitter, should result in HOM interference in the scattering medium. Figure 4(a) shows the measured quantum interference for this circuit which indeed shows a HOM dip (squares). These measurements were done using a pump power of 100 mW and without a bandpass filter. While this higher pump power (in comparison to Fig. 1) generates more photon pairs ( $17 \times 10^6\ \text{s}^{-1}$ ), it also increases the production rate of higher photon-number states. These states reduce the visibility of the HOM dip. The measured HOM dip with a conventional beam splitter at this pump power indeed shows a reduced visibility of 24% (solid curve). To consolidate the quantum nature of the interference [38], we repeated the measurements at a reduced pump power of 40 mW with a bandpass filter in place, which results in a visibility of 59% as shown in Fig. 4(b) (squares). Indeed the data match the prediction and therefore confirms the quantum nature of the interference.

We now explore the programmability of the quantum interference. For indistinguishable single photons and for arbitrary  $\alpha$ , we expect the probability to detect coincidences between output modes  $m$  and  $n$  to scale as  $(1 + \cos \alpha)$ . For instance, setting  $\alpha = 0$  in the patterns on the SLM would double the rate of coincidences compared to the rate obtained for distinguishable photons. This appears as a peak instead of a dip in the measured coincidences as shown in Fig. 4

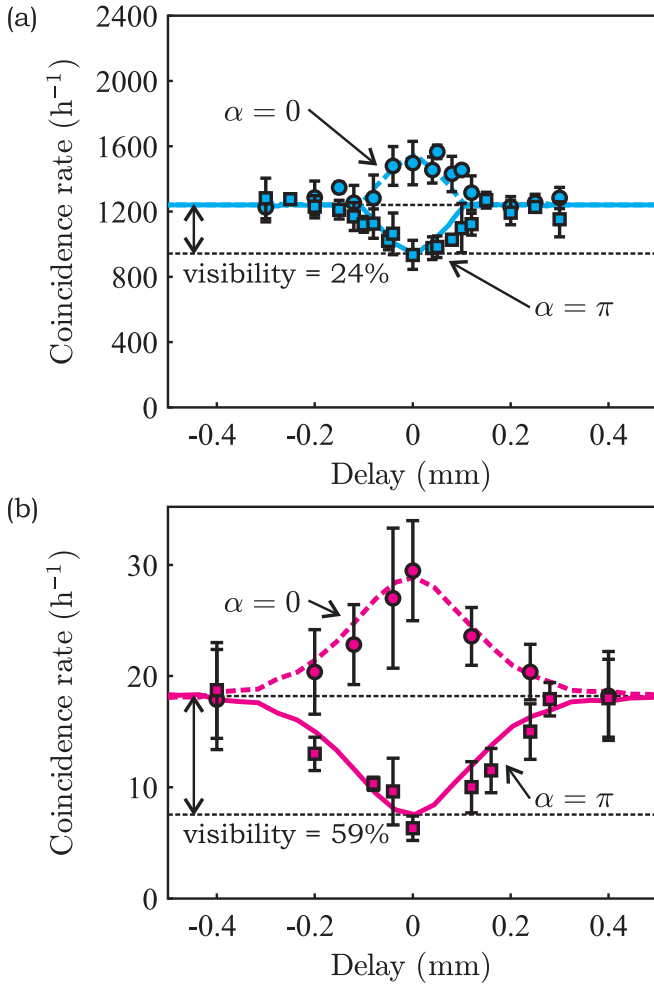


FIG. 4. Programmable quantum interference. Setting  $\alpha = \pi$  gives rise to a dip in coincidence counts (squares), while  $\alpha = 0$  gives a peak (circles). Error bars indicate the standard deviations in the measurements. Panel (a) depicts measurements performed at a pump power of 100 mW without a bandpass filter, and panel (b) at a pump power of 40 mW with the filter in place. The solid curves in the plots correspond to the measured coincidence dips using a conventional beam splitter. The flipped traces of these are shown by the dashed curves as a guide to the eye.

(circles). Although the case with  $\alpha = 0$  can not be realized in a conventional beam splitter, we show flipped traces of the measured HOM dip with a conventional beam splitter as a guide to the eye (dashed curves). Note that the probabilities for bunched photons in the outputs are independent of  $\alpha$ , as is evident from Eq. (3), which makes the output state different from the states typically found when recombining the two outputs from a traditional HOM experiment in a Mach-Zehnder type interferometer [39–41].

Fully programmable quantum interference is demonstrated in our complex scattering medium in Fig. 5. Here the visibility of the quantum interference  $V_0$  is plotted as a function of phase  $\alpha$ . Negative visibility corresponds to a dip in the coincidence counts and positive visibility to a peak. At  $\alpha = 0$  a coincidence peak is observed. The visibility of this peak vanishes at phase  $\alpha = \pi/2$ , after which the visibility increases again as

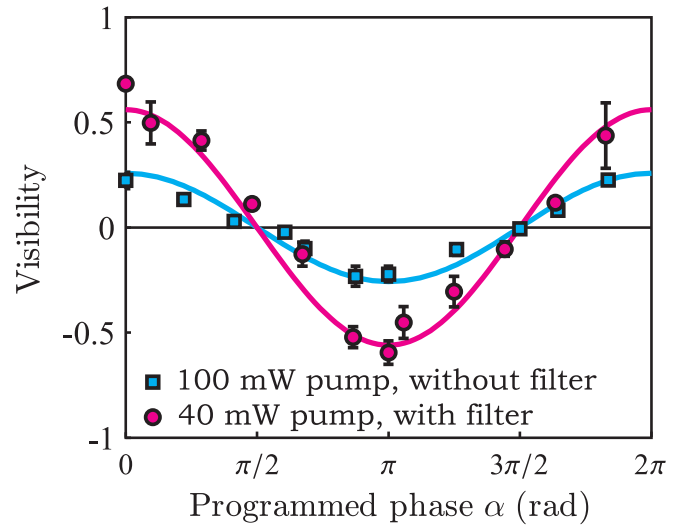


FIG. 5. Programmable quantum interference as a function of programmed phase  $\alpha$  at a pump power of 100 mW without a filter (cyan), and at 40 mW with a bandpass filter (magenta). Error bars indicate the standard deviation in the measurements. The solid curves indicate  $V_0 \cos \alpha$  fits to these data.

a coincidence dip. The well-known HOM dip with a high visibility occurs at phase  $\alpha = \pi$ . The solid curves indicate  $V_0 \cos \alpha$  fits to these data with the prefactor  $V_0$  as the only free parameter.

## V. DISCUSSION

For the measurements at a pump power of 100 mW the average coincidence detection rate is only  $1240 \text{ h}^{-1}$ , corresponding to a single photon detection rate of  $2500 \text{ s}^{-1}$ . This detection rate is small in comparison to the generation rate of  $17 \times 10^6 \text{ s}^{-1}$  as a result of our choice to be deep in the multiple-scattering regime. In this way, we approach the assumption of maximal entropy of the matrix in random-matrix theory [2]. Multimode fibers that were recently exploited for two-photon quantum interference [42] do not provide such a high entropy, since the transmission matrix of a multimode fiber can be transformed into a block-diagonal matrix by a suitable basis [43,44]. We note that having maximal entropy is essential for the application of a scattering medium in quantum-secure authentication [19], which requires a physical unclonable function with a transmission matrix that cannot predictably be approximated by a near-diagonal matrix [45].

In summary, we demonstrated two-photon quantum interference in a high-dimensional linear optical network realized in an opaque scattering medium. Our networks are ideal for quantum information processing [15,16] and boson sampling [6–14]. Excitingly, adaptive control adds programmable functionality to these networks [17,18]. Out of the available channels, we control about  $10^3$  channels to construct a programmable  $2 \times 2$  circuit. In the selected channels, we increase the coincidence detection rates by a factor of  $10^4$ . We have demonstrated that by programming the functionality of this circuit, the well-known Hong-Ou-Mandel bunching can be made to vanish, or be transformed into antibunching.

## ACKNOWLEDGMENTS

We thank Simon Huisman, Thomas Huisman, Ad Lagendijk, Allard Mosk, Boris Škorić, and Tristan Tentrup for discussions and support. This work is financially supported

by Stichting voor Fundamenteel Onderzoek der Materie, Nederlandse Organisatie voor Wetenschappelijk Onderzoek, and Stichting voor de Technische Wetenschappen.

- 
- [1] E. Akkermans and G. Montambaux, *Mesoscopic Physics of Electrons and Photons* (Cambridge University Press, New York, 2007).
- [2] C. W. J. Beenakker, Random-matrix theory of quantum transport, *Rev. Mod. Phys.* **69**, 731 (1997).
- [3] A. P. Mosk, A. Lagendijk, G. Lerosey, and M. Fink, Controlling waves in space and time for imaging and focusing in complex media, *Nat. Photon.* **6**, 283 (2012).
- [4] I. M. Vellekoop and A. P. Mosk, Focusing coherent light through opaque strongly scattering media, *Opt. Lett.* **32**, 2309 (2007).
- [5] S. M. Popoff, A. Goetschy, S. F. Liew, A. D. Stone, and H. Cao, Coherent Control of Total Transmission of Light through Disordered Media, *Phys. Rev. Lett.* **112**, 133903 (2014).
- [6] S. Aaronson and A. Arkhipov, The computational complexity of linear optics, in *Proceedings of the ACM Symposium on Theory of Computing '11* (ACM, New York, 2011), p. 333.
- [7] A. Peruzzo, M. Lobino, J. C. F. Matthews, N. Matsuda, A. Politi, K. Poulios, X.-Q. Zhou, Y. Lahini, N. Ismail, K. Wörhoff, Y. Bromberg, Y. Silberberg, M. G. Thompson, and J. L. O'Brien, Quantum walks of correlated photons, *Science* **329**, 1500 (2010).
- [8] A. M. Childs, D. Gosset, and Z. Webb, Universal computation by multiparticle quantum walk, *Science* **339**, 791 (2013).
- [9] M. A. Broome, A. Fedrizzi, S. Rahimi-Keshari, J. Dove, S. Aaronson, T. C. Ralph, and A. G. White, Photonic boson sampling in a tunable circuit, *Science* **339**, 794 (2013).
- [10] J. B. Spring, B. J. Metcalf, P. C. Humphreys, W. S. Kolthammer, X.-M. Jin, M. Barbieri, A. Datta, N. Thomas-Peter, N. K. Langford, D. Kundys, J. C. Gates, B. J. Smith, P. G. R. Smith, and I. A. Walmsley, Boson sampling on a photonic chip, *Science* **339**, 798 (2013).
- [11] M. Tillmann, B. Daki, R. Heilmann, S. Nolte, A. Szameit, and P. Walther, Experimental boson sampling, *Nat. Photon.* **7**, 540 (2013).
- [12] A. Crespi, R. Osellame, R. Ramponi, D. J. Brod, E. F. Galvo, N. Spagnolo, C. Vitelli, E. Maiorino, P. Mataloni, and F. Sciarrino, Integrated multimode interferometers with arbitrary designs for photonic boson sampling, *Nat. Photon.* **7**, 545 (2013).
- [13] N. Spagnolo, C. Vitelli, M. Bentivegna, D. J. Brod, A. Crespi, F. Flamini, S. Giacomini, G. Milani, R. Ramponi, P. Mataloni, R. Osellame, E. F. Galvão, and F. Sciarrino, Experimental validation of photonic boson sampling, *Nat. Photon.* **8**, 615 (2014).
- [14] J. Carolan, J. D. A. Meinecke, P. J. Shadbolt, N. J. Russell, N. Ismael, K. Wörhoff, T. Rudolph, M. G. Thompson, J. L. O'Brien, J. C. F. Matthews, and A. Laing, On the experimental verification of quantum complexity in linear optics, *Nat. Photon.* **8**, 621 (2014).
- [15] E. Knill, R. Laflamme, and G. J. Milburn, A scheme for efficient quantum computation with linear optics, *Nature (London)* **409**, 46 (2001).
- [16] P. Kok, W. J. Munro, K. Nemoto, T. C. Ralph, J. P. Dowling, and G. J. Milburn, Linear optical quantum computing with photonic qubits, *Rev. Mod. Phys.* **79**, 135 (2007).
- [17] J. Carolan, C. Harrold, C. Sparrow, E. Martín-López, N. J. Russell, J. W. Silverstone, P. J. Shadbolt, N. Matsuda, M. Oguma, M. Itoh, G. D. Marshall, M. G. Thompson, J. C. F. Matthews, T. Hashimoto, J. L. O'Brien, and A. Laing, Universal linear optics, *Science* **349**, 711 (2015).
- [18] N. C. Harris, G. R. Steinbrecher, J. Mower, Y. Lahini, M. Prabhu, T. Baehr-Jones, M. Hochberg, S. Lloyd, and D. Englund, Bosonic transport simulations in a large-scale programmable nanophotonic processor, [arXiv:1507.03406](https://arxiv.org/abs/1507.03406) [quant-ph].
- [19] S. A. Goorden, M. Horstmann, A. P. Mosk, B. Škorić, and P. W. H. Pinkse, Quantum-secure authentication of a physical unclonable key, *Optica* **1**, 421 (2014).
- [20] C. W. J. Beenakker, J. W. F. Venderbos, and M. P. van Exter, Two-Photon Speckle as a Probe of Multi-Dimensional Entanglement, *Phys. Rev. Lett.* **102**, 193601 (2009).
- [21] W. H. Peeters, J. J. D. Moerman, and M. P. van Exter, Observation of Two-Photon Speckle Patterns, *Phys. Rev. Lett.* **104**, 173601 (2010).
- [22] P. Lodahl, A. P. Mosk, and A. Lagendijk, Spatial Quantum Correlations in Multiple Scattered Light, *Phys. Rev. Lett.* **95**, 173901 (2005).
- [23] P. Lodahl and A. Lagendijk, Transport of Quantum Noise through Random Media, *Phys. Rev. Lett.* **94**, 153905 (2005).
- [24] S. Smolka, A. Huck, U. L. Andersen, A. Lagendijk, and P. Lodahl, Observation of Spatial Quantum Correlations Induced by Multiple Scattering of Nonclassical Light, *Phys. Rev. Lett.* **102**, 193901 (2009).
- [25] T. J. Huisman, S. R. Huisman, A. P. Mosk, and P. W. H. Pinkse, Controlling single-photon Fock-state propagation through opaque scattering media, *Appl. Phys. B* **116**, 603 (2014).
- [26] H. Defienne, M. Barbieri, B. Chalopin, B. Chatel, I. A. Walmsley, B. J. Smith, and S. Gigan, Nonclassical light manipulation in a multiple-scattering medium, *Opt. Lett.* **39**, 6090 (2014).
- [27] S. R. Huisman, T. J. Huisman, S. A. Goorden, A. P. Mosk, and P. W. H. Pinkse, Programming balanced optical beam splitters in white paint, *Opt. Express* **22**, 8320 (2014).
- [28] S. R. Huisman, T. J. Huisman, T. A. W. Wolterink, A. P. Mosk, and P. W. H. Pinkse, Programmable multiport optical circuits in opaque scattering materials, *Opt. Express* **23**, 3102 (2015).
- [29] C. K. Hong, Z. Y. Ou, and L. Mandel, Measurement of Subpicosecond Time Intervals between Two Photons by Interference, *Phys. Rev. Lett.* **59**, 2044 (1987).
- [30] S. R. Huisman, N. Jain, S. A. Babichev, F. Vewinger, A. N. Zhang, S. H. Youn, and A. I. Lvovsky, Instant single-photon Fock state tomography, *Opt. Lett.* **34**, 2739 (2009).
- [31] E. Bimbard, N. Jain, A. MacRae, and A. I. Lvovsky, Quantum-optical state engineering up to the two-photon level, *Nat. Photon.* **4**, 243 (2010).
- [32] See Supplemental Material at <http://link.aps.org/supplemental/10.1103/PhysRevA.93.053817> for details about the spontaneous parametric down-conversion source and the estimate of enhanced coincidence rates.

- [33] J. W. Goodman, Some fundamental properties of speckle\*, *J. Opt. Soc. Am.* **66**, 1145 (1976).
- [34] J. Li, G. Yao, and L. V. Wang, Degree of polarization in laser speckles from turbid media: Implications in tissue optics, *J. Biomed. Opt.* **7**, 307 (2002).
- [35] Y. Guan, O. Katz, E. Small, J. Zhou, and Y. Silberberg, Polarization control of multiply scattered light through random media by wavefront shaping, *Opt. Lett.* **37**, 4663 (2012).
- [36] S. M. Barnett, J. Jeffers, A. Gatti, and R. Loudon, Quantum optics of lossy beam splitters, *Phys. Rev. A* **57**, 2134 (1998).
- [37] M. Patra and C. W. J. Beenakker, Propagation of squeezed radiation through amplifying or absorbing random media, *Phys. Rev. A* **61**, 063805 (2000).
- [38] R. Ghosh and L. Mandel, Observation of Nonclassical Effects in the Interference of Two Photons, *Phys. Rev. Lett.* **59**, 1903 (1987).
- [39] J. G. Rarity, P. R. Tapster, E. Jakeman, T. Larchuk, R. A. Campos, M. C. Teich, and B. E. A. Saleh, Two-Photon Interference in a Mach-Zehnder Interferometer, *Phys. Rev. Lett.* **65**, 1348 (1990).
- [40] J. Chen, K. F. Lee, and P. Kumar, Deterministic quantum splitter based on time-reversed Hong-Ou-Mandel interference, *Phys. Rev. A* **76**, 031804(R) (2007).
- [41] J. W. Silverstone, D. Bonneau, K. Ohira, N. Suzuki, H. Yoshida, N. Iizuka, M. Ezaki, C. M. Natarajan, M. G. Tanner, R. H. Hadfield, V. Zwiller, G. D. Marshall, J. G. Rarity, J. L. O'Brien and M. G. Thompson, On-chip quantum interference between silicon photon-pair sources, *Nat. Photon.* **8**, 104 (2014).
- [42] H. Defienne, M. Barbieri, I. A. Walmsley, B. J. Smith, and S. Gigan, Two-photon quantum walk in a multimode fiber, *Sci. Adv.* **2**, e1501054 (2016).
- [43] J. Carpenter, B. J. Eggleton, and J. Schröder, 110×110 optical mode transfer matrix inversion, *Opt. Express* **22**, 96 (2014).
- [44] M. Plöschner, T. Tyc, and T. Čížmár, Seeing through chaos in multimode fibres, *Nat. Photon.* **9**, 529 (2015).
- [45] R. Pappu, B. Recht, J. Taylor, and N. Gershenfeld, Physical one-way functions, *Science* **297**, 2026 (2002).